Inorg. Chem. **2006**, *45*, 7821–7827

Inorganic Chemistry
Article

Synthesis, Crystal Structures, and Magnetic Properties of Cyano-Bridged Honeycomblike Layers M^{V}–Cu^{II} (M = Mo, W) Chelated by a Macrocyclic Ligand

Jeong Hak Lim,[†] Jun Sung Kang,[‡] Hyoung Chan Kim,[§] Eui Kwan Koh,[‡] and Chang Seop Hong*,[†]

Department of Chemistry and Center for Electro- and Photo-Responsive Molecules, Korea University, Seoul 136-701, Korea, Nano-Bio System Research Team, Korea Basic Science Institute, Seoul 136-713, Korea, and Systems Research Team, Research & Development Division, Nuclear Fusion Research Center, Daejeon 305-333, Korea

Received May 19, 2006

Two cyano-bridged Cu^{II}–M^{V} [M = Mo (**2**), W (**3**)] complexes formed by self-assembly of octacyanometalates $[M(CN)_8]^{3-}$ (M = Mo, W) with a new molecular precursor $[Cu(L2)]^{2+}$ (**1**) (L2 = a macrocyclic ligand) in a 2:3 ratio have been investigated in terms of structures and magnetic behaviors. The M_2Cu_3 repeating unit of both bimetallic compounds is extended to a two-dimensional honeycomblike layered structure. The pendant ethyl groups on L2 noticeably influence the structural parameters around the Cu center. Compared with the system composed of a macrocycle without a side group, Cu–N_{ax} (ax = axial) distances become shorter and the Cu–N_{ax}-C_{ax} angles are more bent for **2** and **3**. The magnetic data denote that the Cu(II) and M(V) spins undergo explicit ferromagnetic interactions via CN bridges. From a structural and magnetic point of view, given that the Cu–N_{ax} bond length in the tetragonally distorted octahedral Cu(II) environment is long enough, the overall ferromagnetic character remains despite the variation of Cu–N_{ax}–C_{ax} angle in this system.

Introduction

Molecule-based magnetic materials have attracted much attention because of their potential applications in magnetic devices.[1] Hexacyanometalates $[A(CN)_6]^{n-}$ (A = Cr, Mn, Fe, etc.), as building blocks, have been extensively studied,[2] and bimetallic assemblies with multidimensional structures have shown not only spontaneous magnetization at high T_C[3] but also appealing properties concerning magneto-chiral dichroism,[4] photomagnetic effects,[5] and porous metal−organic frameworks.[6]

Recently, the frequent use of octacyanometalates $[B(CN)_8]^{n-}$ (B = 4d or 5d metal ions) as appropriate synthons for magnetic coordination polymers stems from the merits of the strong magnetic interactions induced by their diffuse orbitals, diverse geometric structures, and photoresponsive features.[7] In particular, a number of bimetallic assemblies based on $[M(CN)_8]^{3-}$ (M = Mo, W) exhibiting intriguing magnetic and other properties have been synthesized and characterized. These compounds are formed by self-assembly of $[M(CN)_8]^{3-}$ with divalent metal ions of Mn(II),[8] Co(II),[9] Ni(II),[10] and Cu(II)[11] occupied by ancillary ligands. Their structures vary from discrete molecules, one-dimensional (1D) chains, and 2D layers to 3D frameworks.[8−11]

For octacyanometalate-based Cu−M (M = Mo, W) bimetallic systems, the magnetic properties may be governed

---

* To whom correspondence should be addressed. E-mail: cshong@korea.ac.kr.

[†] Korea University.

[‡] Korea Basic Science Institute.

[§] Nuclear Fusion Research Center.

(1) Turnbull, M. M.; Sugimoto, T.; Thompson, L. K. *Molecule-Based Magnetic Materials*; American Chemical Society: Washington, DC, 1996.

(2) Ohba, M.; Okawa, H. *Coord. Chem. Rev.* **2000**, *198*, 313.

(3) (a) Kou, H.-Z.; Gao, S.; Zhang, J.; Wen, G.-H.; Su, G.; Zheng, R. K.; Zhang, X. X. *J. Am. Chem. Soc.* **2001**, *123*, 11809. (b) Ohba, M.; Usuki, N.; Fukita, N.; Okawa, H. *Angew. Chem., Int. Ed. Engl.* **1999**, *38*, 1795.

(4) (a) Imai, H.; Inoue, K.; Kikuchi, K.; Yoshida, Y.; Ito, M.; Sunahara, T.; Onaka, S. *Angew. Chem., Int. Ed.* **2004**, *43*, 5618. (b) Inoue, K.; Imai, H.; Ghalsasi, P. S.; Kikuchi, K.; Ohba, M.; Okawa, H.; Yakhmi, J. V. *Angew. Chem., Int. Ed.* **2001**, *40*, 4242.

(5) Sato, O.; Iyoda, T.; Fujishima, A.; Hashimoto, K. *Science* **1996**, *272*, 704.

(6) (a) Kaye, S. S.; Long, J. R. *J. Am. Chem. Soc.* **2005**, *127*, 6506. (b) Beauvais, L. G.; Long, J. R. *J. Am. Chem. Soc.* **2002**, *124*, 12096.

(7) (a) Arimoto, Y.; Ohkoshi, S.-i.; Zhong, Z. J.; Seino, H.; Mizobe, Y.; Hashimoto, K. *J. Am. Chem. Soc.* **2003**, *125*, 9240. (b) Pradhan, R.; Desplanches, C.; Guionneau, P.; Sutter, J.-P. *Inorg. Chem.* **2003**, *42*, 6607. (c) Bennett, M. V.; Long, J. R. *J. Am. Chem. Soc.* **2003**, *125*, 2394.

10.1021/ic060868b CCC: $33.50

by orbital consideration: the overlap between the M dπ and Cu dσ orbitals results in ferromagnetic interactions caused by orbital orthogonality, while the overlap between the M dπ and Cu dπ orbitals favors antiferromagnetic couplings.[11,12] However, the magnetic consequences in the latter are not well established. To probe the magnetic-exchange nature between paramagnetic centers for the latter, it is necessary to control specific binding sites for bridging units. A rational design for a model system of interest is to confine the coordination sphere by reserving preprogrammed locations for incoming bridges. Our efforts to this end have been to employ octahedral Cu(II) complexes blocked by suitable tetradentate macrocyclic ligands in which four equatorial positions are filled by nitrogen atoms from a macrocycle and two axial sites are weakly bound by good leaving groups. In this line, octacyanometalate-based Cu(II)−M(V) compounds with 1D or 2D structures, in which the Cu ions are surrounded by macrocyclic ligands, were investigated, indicating that global ferromagnetic interactions take place among Cu(II) and M(V) spins.[12] The structural parameters around the Cu centers can be subtly modulated by accommodating side groups on macrocycles. To scrutinize the genuine magnetic character between Cu(II) and M(V) through the axial CN linkage, we have extended our work to choose a macrocyclic ligand that has a bulky side group capable of altering structural features.

Herein, we report the syntheses, crystal structures, and magnetic characterization of two unique honeycomblike sheets $[Cu(L2)]_3[Mo(CN)_8]_2\cdot6H_2O\cdot2MeOH$ (**2**$\cdot6H_2O\cdot2MeOH$) and $[Cu(L2)]_3[W(CN)_8]_2\cdot6H_2O\cdot2MeOH$ (**3**$\cdot6H_2O\cdot2MeOH$) self-assembled using $[M(CN)_8]^{3-}$ (M = Mo, W) and a new molecular precursor $[Cu(L2)(ClO_4)_2]$ (**1**) with ethyl side groups on the macrocyclic ring. The pendant groups render the $Cu-N_{ax}$ (ax = axial) bond length shorter and the Cu−NC angle more bent than those of the Cu(II)−Mo(V) system with cyclam (cyclam = 1,4,8,11-tetraazacyclotetradecane) containing no side groups.[12a] Magnetic data reveal that the Cu(II) and M(V) ions interact ferromagnetically through the CN ligand. From structural and magnetic considerations, when the $Cu-N_{ax}$ distance is long enough, the ferromagnetic nature remains dominant even though the $Cu-N_{ax}-C_{ax}$ angle varies.

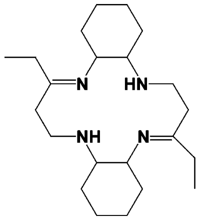

L1

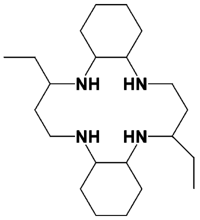

L2

Experimental Section

Reagent. $(Bu_4N)_3[M(CN)_8]$ (M = Mo, W) was prepared according to the literature procedure.[13] All the other chemicals and solvents in the synthesis were of reagent grade and used as received. All manipulations were performed under aerobic conditions.

Synthesis. ***Caution:*** *Perchlorate salts of metal compounds with organic ligands are potentially explosive. Only small amounts of material should be cautiously handled.*

L1$\cdot$2HClO$_4$. Perchloric acid (60%, 3.57 mL) was added dropwise to an ice-cooled EtOH (30 mL) solution of 1,2-diaminocyclohexane (5.0 mL). Ethyl vinyl ketone (4.1 mL) was slowly treated in an ice bath, and the color of the solution was changed from clear yellow to deep brown. The resultant solution was stirred at room temperature for 3 days. The final product was filtered off, washed with EtOH, and dried in a vacuum. Yield: 12%. Anal. Calcd for $C_{22}H_{42}Cl_2N_4O_8$: C, 47.1; H, 7.54; N, 9.98. Found: C, 47.2; H, 7.33; N, 10.4.

L2. NaOH (0.16 g) and $NaBH_4$ (0.18 g) were added over 2 h to a methanolic solution (5 mL) of L1$\cdot$2HClO$_4$ (1.0 g) in an ice bath. The mixture was stirred at room temperature for 2 h and refluxed for 20 min. The filtrate was treated with NaOH (0.48 g) in water and stirred for 10 min. The white solid was filtered off, washed with H_2O, and dried in a vacuum over P_2O_5. Yield: 88%. Anal. Calcd for $C_{22}H_{34}N_4$: C, 72.4; H, 12.2; N, 15.4. Found: C, 72.0; H, 11.8; N, 15.6.

$[Cu(L2)(ClO_4)_2]$ (1). A methanolic solution (75 mL) of $Cu(OAc)_2\cdot H_2O$ (2.8 mmol) and L2 (2.8 mmol) was heated at reflux for 1 h and cooled to room temperature. The addition of $NaClO_4$ (5.6 mmol) to the solution produced precipitates immediately. The product was collected by filtration, washed with MeOH, and dried in air. Red single crystals were obtained by recrystallizing the solid in MeCN/ether. Yield: 88%. Anal. Calcd for $C_{11}H_{22}ClCu_{0.5}N_2O_4$: C, 42.1; H, 7.07; N, 8.93. Found: C, 41.9; H, 7.05; N, 8.62.

Compound 2. A methanolic solution of $(Bu_4N)_3[Mo(CN)_8]$ (0.10 mmol) was added with stirring to **1** (0.15 mmol) dissolved in MeCN/H_2O (5:1). The filtered solution was left undisturbed in the dark, forming pale brown crystals in a yield of 80%. The dried product was analyzed as **2**$\cdot6H_2O$. Anal. Calcd for $C_{82}H_{144}Cu_3Mo_2N_{28}O_6$: C, 49.2; H, 7.25; N, 19.6. Found: C, 49.6; H, 6.79; N, 19.9.

Compound 3. A methanolic solution of $(Bu_4N)_3[W(CN)_8]$ (0.10 mmol) was added to **1** (0.15 mmol) dissolved in MeCN/H_2O (5:1).

---

(8) (a) Larionova, J.; Gross, M.; Pilkington, M.; Andres, H.; Stoeckli-Evans, H.; Gudel, H. U.; Decurtins, S. *Angew. Chem., Int. Ed.* **2000**, *39*, 1605. (b) Zhong, Z. J.; Seino, H.; Mizobe, Y.; Hidai, M.; Fujishima, A.; Ohkosh, S.-i.; Hashimoto, K. *J. Am. Chem. Soc.* **2000**, *122*, 2952. (c) Zhong, Z. J.; Seino, H.; Mizobe, Y.; Hidai, M.; Verdaguer, M.; Ohkoshi, S.-i.; Hashimoto, K. *Inorg. Chem.* **2000**, *39*, 5095. (d) Kashiwagi, T.; Ohkoshi, S.-i.; Seino, H.; Mizobe, Y.; Hashimoto, K. *J. Am. Chem. Soc.* **2004**, *126*, 5024. (e) Podgajny, R.; Desplanches, C.; Sieklucka, B.; Sessoli, R.; Villar, V.; Paulsen, C.; Wernsdorfer, W.; Dromzée, Y.; Verdaguer, M. *Inorg. Chem.* **2002**, *41*, 1323. (f) Li, D.-f.; Gao, S.; Zheng, L.-m.; Tang, W.-x. *J. Chem. Soc., Dalton Trans.* **2002**, 2805.

(9) (a) Li, D.; Zheng, L.; Zhang, Y.; Huang, J.; Gao, S.; Tang, W. *Inorg. Chem.* **2003**, *42*, 6123. (b) Song, Y.; Zhang, P.; Ren. X.-M.; Shen, X.-F.; Li, Y.-Z.; You, X.-Z. *J. Am. Chem. Soc.* **2005**, *127*, 3708.

(10) Bonadio, F.; Gross, M.; Stoeckli-Evans, H.; Decurtins, S. *Inorg. Chem.* **2002**, *41*, 5891.

(11) (a) Korzeniak, T.; Stadnicka, K.; Rams, M.; Sieklucka, B. *Inorg. Chem.* **2004**, *43*, 4811. (b) Korzeniak, T.; Podgajny, R.; Alcock, N. W.; Lewinski, K.; Balanda, M.; Wasiutynski, T.; Sieklucka, B. *Polyhedron* **2003**, *22*, 2183. (c) Ohkoshi, S.-i.; Arimoto, Y.; Hozumi, T.; Seino, H.; Mizobe, Y.; Hashomoto, K. *Chem. Commun.* **2003**, 2772. (d) Podgajny, R.; Korzeniak, T.; Balanda, M.; Wasiutynski, T.; Errington, W.; Kemp, T. J.; Alcock, N. W.; Sieklucka, B. *Chem. Commun.* **2002**, 1138. (e) Li, D.-f.; Zheng, L.-m.; Wang, X.-y.; Huang, J.; Gao, S.; Tang, W.-x. *Chem. Mater.* **2003**, *15*, 2094. (f) Korzeniak, T.; Stadnicka, K.; Pelka, R.; Balanda, M.; Tomala, K.; Kowalski, K.; Sieklucka, B. *Chem. Commun.* **2005**, 2939.

(12) (a) You, Y. S.; Kim, D.; Do, Y.; Oh, S. J.; Hong, C. S. *Inorg. Chem.* **2004**, *43*, 6899. (b) You, Y. S.; Yoon, J. H.; Lim, J. H.; Kim, H. C.; Hong, C. S. *Inorg. Chem.* **2005**, *44*, 7063.

(13) Pribush, R. A.; Archer, R. D. *Inorg.* Chem. **1974**, *13*, 2556.

Table 1. Crystallographic Data for **1**−**3**

	1	**2**·$6H_2O$·2MeOH	**3**·$6H_2O$·2MeOH
formula	$C_{11}H_{22}ClCu_{0.50}N_2O_4$	$C_{42}H_{76}Cu_{1.5}MoN_{14}O_4$	$C_{42}H_{76}Cu_{1.5}N_{14}O_4W$
fw	313.53	1032.42	1120.33
cryst syst	monoclinic	triclinic	triclinic
space group	$P2_1/n$	$P\bar{1}$	$P\bar{1}$
temp (K)	298	130	130
a (Å)	9.2736(2)	10.3001(2)	10.3034(2)
b (Å)	11.6867(2)	16.3346(4)	16.2949(3)
c (Å)	13.0068(2)	16.4319(4)	16.4554(3)
α (deg)	90	74.3290(10)	74.4490(10))
β (deg)	96.4030(10)	86.3890(10)	86.0210(10)
γ (deg)	90	78.1000(10)	78.3160(10)
V ($Å^3$)	1400.85(4)	2604.59(10)	2606.12(8)
Z	4	2	2
d_{calcd} (g cm^{-3})	1.487	1.316	1.428
μ (mm^{-1})	1.021	0.899	2.863
F(000)	662	1087	1151
θ range (deg)	2.35−28.33	1.29−28.27	1.28−28.28
reflns collected	13 367	41 992	43 256
unique reflns	3459	12 715	12 743
params	170	571	571
$R1^{a}$ [$I > 2\sigma(I)$]	0.0404	0.0493	0.0396
$wR2^{b}$ [$I > 2\sigma(I)$]	0.1132	0.1378	0.1056

[a] $R1 = \sum||F_o| - |F_c||/\sum|F_c|$. [b] $wR2 = [\sum w(F_o^2 - F_c^2)^2/\sum w(F_o^2)^2]^{1/2}$.

After it was stirred for a few minutes, the resulting solution was filtered. The filtrate was allowed to stand undisturbed in the dark, giving violet crystals in a yield of 79%. The dried solid was analyzed as **3**·$6H_2O$·MeOH. Anal. Calcd for $C_{84}H_{148}Cu_3N_{28}O_7W_2$: C, 44.8; H, 6.75; N, 17.7. Found: C, 45.1; H, 6.28; N, 17.7.

Physical Measurements. Elemental analyses for C, H, and N were performed at the Elemental Analysis Service Center of Sogang University. Infrared spectra were obtained from KBr pellets with a Bomen MB-104 spectrometer. Magnetic susceptibility data for **2** and **3** were carried out using a Quantum Design MPMS-7 SQUID susceptometer. Diamagnetic corrections of **2** and **3** were estimated from Pascal's Tables.

Crystallographic Structure Determination. X-ray data for **1**−**3** were collected on a Bruker SMART APEXII diffractometer equipped with graphite-monochromated Mo Kα radiation (λ = 0.71073 Å). The reflection data were corrected for Lorentz and polarization factors. The structures were solved by direct (**1**) or Patterson (**2** and **3**) methods and refined by full-matrix least-squares analysis using anisotropic thermal parameters for non-hydrogen atoms with the SHELXTL program.[14] All hydrogen atoms except for the hydrogens bound to water or MeOH molecules were calculated at idealized positions and refined with the riding models. Crystallographic data and the details of data collection are listed in Table 1.

Results and Discussion

Synthesis and Characterization. The IR data for **1** exhibit a NH stretching of secondary amines evident at 3207s cm^{-1}. The characteristic bands for perchlorate anions are observed as strong multiple peaks in the range of 1086−1143 cm^{-1}. Compounds **2** and **3** were prepared by treating $[Cu(L2)]^{2+}$ with $[M(CN)_8]^{3-}$ in a stoichiometric ratio of 3:2. Two perchlorate anions coordinated to a Cu center of **1** were replaced by the nitrogen atoms of CN ligands among the precursor $[M(CN)_8]^{3-}$, generating neutral coordination polymers of **2** and **3**. The reaction progress was checked by the absence of the perchlorate peaks in the IR spectrum. The CN stretching vibrations are present at 2145m and 2156m (sh) cm^{-1} for **2** and 2143m and 2151m cm^{-1} for **3**. On the basis of the reference CN peaks centered at 2140m and 2123m cm^{-1} for $(Bu_4N)_3Mo(CN)_8$ and 2141m, 2130m, and 2123m (sh) cm^{-1} for $(Bu_4N)_3W(CN)_8$, the peaks at 2156m (**2**) and 2151m cm^{-1} (**3**), which shift toward higher frequencies than the references, are assigned to bridging CN groups, while the bands at 2140m (**2**) and 2143m cm^{-1} (**3**) involve unbound CN ligands in the $[M(CN)_8]^{3-}$ unit. There are broad bands around 3466 cm^{-1} in **2** and around 3500 cm^{-1} in **3**, which can be attributed to the OH stretchings of lattice water molecules, implying the existence of hydrogen bonds. For secondary amines, NH stretchings appear at 3227s and 3171s cm^{-1} for **2** and 3243s, 3227s (sh), and 3174m (br) cm^{-1} for **3**. The advent of more than two peaks for the secondary NH groups, compared to the IR band of the NH moiety in **1**, shows that hydrogen bonds are involved.

Description of the Structures. An ORTEP diagram of **1** is illustrated in Figure 1. Selected bond distances and angles are summarized in Table 2. The Cu atom in an inversion

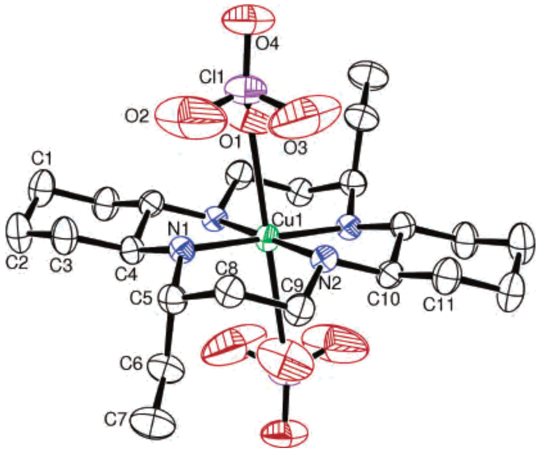

Figure 1. ORTEP diagram of **1** with the atom-labeling scheme.

---

(14) Sheldrick, G. M. *SHELXTL*, version 5; Bruker AXS: Madison, WI, 1995.

Table 2. Bond Lengths (Å) and Angles (deg) for **1**[a]

Cu(1)−N(2)	2.0164(18)	Cu(1)−N(2)^{i}	2.0164(18)
Cu(1)−N(1)^{i}	2.0403(17)	Cu(1)−N(1)	2.0403(17)
N(2)−Cu(1)−N(2)^{i}	180.0	N(2)−Cu(1)−N(1)^{i}	85.06(7)
N(2)^{i} −Cu(1)−N(1)^{i}	94.94(7)	N(2)−Cu(1)−N(1)	94.94(7)
N(2)^{i} −Cu(1)−N(1)	85.06(7)	N(1)^{i} −Cu(1)−N(1)	180.0
N(4)−N(1)−Cu(1)	108.19(12)	C(5)−N(1)−Cu(1)	121.42(14)
C(9)−N(2)−Cu(1)	116.80(15)	C(10)−N(2)−Cu(1)	108.03(13)

[a] Symmetry transformations used to generate equivalent atoms: (i) −*x*, −*y* + 2, −*z* + 1.

center adopts a distorted octahedral geometry, consisting of four equatorial N donors of the macrocyclic ligand (L2) with an average Cu−N length of 2.03(1) Å and two axial O atoms of perchlorate anions with a significant tetragonal elongation (Cu−O1 = 2.762(3) Å) resulting from the Jahn−Teller effect of a octahedral Cu(II) ion. The macrocycle forms two five-membered rings and two six-membered rings with the metal center. The six-membered chelate rings possess a chair conformation, and the five-membered-rings appear to be in a gauche conformation. The bite distance (2.989(3) Å) of the six-membered rings is larger than that (2.742(3) Å) of the five-membered rings. The bite angles of the six- and five-membered rings are 94.94(7) and 85.06(7)°. These values are typical of those for the six- and five-membered chelate rings in compounds coordinated by a 14-membered macrocyclic ligand.[15] The macrocycle L2 can be described as a R,R,S,S-configuration in which the orientation of the two hydrogen atoms of the secondary amines connected to the Cu(II) center is opposite to that of the other two hydrogen atoms, allowing the thermodynamically most stable arrangement. The pendant groups (C5−C6) are positioned almost perpendicular to the CuN$_4$ basal plane, which can affect the coordination patterns of incoming CN ligands. The hydrogen atoms of the secondary amines undergo hydrogen bonds with oxygen atoms of the perchlorate anions (N1−H1···O2 = 3.162(4) Å, ∠N1H1O2 = 162°; N2−H2···O3 = 3.059(5) Å, ∠N2H2O3 = 157°).

Compound **2**, which is isostructural with **3**, crystallizes in the triclinic crystal system with the space group $P\bar{1}$. The representative structural view of **2** with the selected atom-numbering scheme is shown in Figure 2. Selected bond distances and angles of **2** and **3** are given in Tables 3 and 4, respectively. Each asymmetric unit of **2** and **3** is composed of two [M(CN)$_8$]$^{3-}$ (M = Mo, W) anions and three [Cu(L2)]$^{2+}$ cations. The central geometry around M adopts a distorted square antiprism. The M center is coordinated by eight CN groups with average M1−C bond distances of 2.155(8) Å for **2** and 2.161(10) Å for **3**. The bridging M−C−N angles remain almost linear with maximum deviations from linearity of 4.8 (**2**) and 4.9° (**3**), respectively, which are in the normal range of the related systems.[8−11] Three CN groups of the [M(CN)$_8$]$^{3-}$ unit bridge neighboring Cu(II) atoms with distances of 5.5551(3) Å for Mo1−Cu1, 5.4987(3) Å for Mo1−Cu2, and 5.4552(3) Å for Mo1−Cu3, which are quite similar to those of 5.5495(2) Å for W1−Cu1, 5.5041(2) Å for W1−Cu2, and 5.4576(2) Å for W1−Cu3.

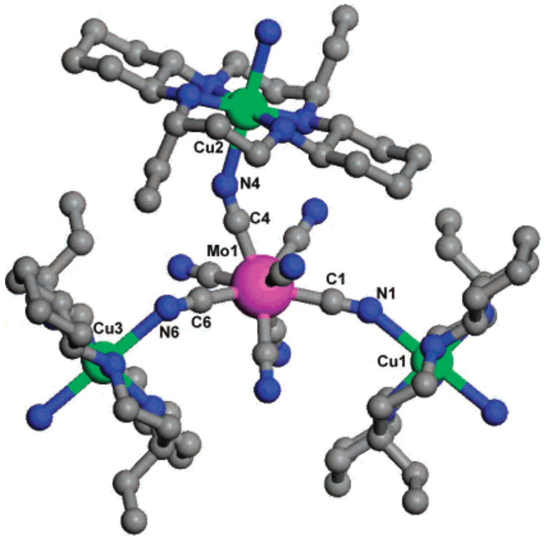

Figure 2. Molecular view of **2**: C, gray; N, blue; Cu, green; Mo, pink.

Table 3. Bond Lengths (Å) and Angles (deg) for **2**[a]

Mo(1)−C(1)	2.145(3)	Mo(1)−C(6)	2.146(4)
Mo(1)−C(4)	2.150(3)	Mo(1)−C(3)	2.156(4)
Mo(1)−C(8)	2.157(3)	Mo(1)−C(5)	2.157(4)
Mo(1)−C(2)	2.162(3)	Mo(1)−C(7)	2.168(3)
N(1)−Cu(1)	2.416(3)	N(4)−Cu(2)	2.466(3)
Cu(1)−N(9)	2.019(3)	Cu(1)−N(10)	2.053(3)
Cu(2)−N(12)	2.023(2)	Cu(2)−N(11)	2.065(3)
Cu(3)−N(14)	2.017(3)	Cu(3)−N(13)	2.056(3)
Cu(3)−N(6)	2.515(5)		
C(1)−Mo(1)−C(6)	141.19(15)	C(1)−Mo(1)−C(4)	121.13(14)
C(6)−Mo(1)−C(4)	76.40(13)	C(1)−Mo(1)−C(3)	73.45(18)
C(6)−Mo(1)−C(3)	79.99(19)	C(4)−Mo(1)−C(3)	74.35(15)
C(1)−Mo(1)−C(8)	76.73(14)	C(6)−Mo(1)−C(8)	113.50(15)
C(4)−Mo(1)−C(8)	139.72(13)	C(3)−Mo(1)−C(8)	144.17(15)
C(1)−Mo(1)−C(5)	141.12(15)	C(6)−Mo(1)−C(5)	73.91(17)
C(4)−Mo(1)−C(5)	74.66(15)	C(3)−Mo(1)−C(5)	143.24(18)
C(8)−Mo(1)−C(5)	71.52(14)	C(1)−Mo(1)−C(2)	72.31(12)
C(6)−Mo(1)−C(2)	143.74(13)	C(4)−Mo(1)−C(2)	71.42(12)
C(3)−Mo(1)−C(2)	106.35(14)	C(8)−Mo(1)−C(2)	82.57(13)
C(5)−Mo(1)−C(2)	81.76(14)	C(1)−Mo(1)−C(7)	75.12(12)
C(6)−Mo(1)−C(7)	72.39(13)	C(4)−Mo(1)−C(7)	141.81(12)
C(3)−Mo(1)−C(7)	78.99(13)	C(8)−Mo(1)−C(7)	74.51(12)
C(5)−Mo(1)−C(7)	115.90(13)	C(2)−Mo(1)−C(7)	143.61(12)
N(1)−C(1)−Mo(1)	178.5(3)	C(1)−N(1)−Cu(1)	153.8(3)
N(2)−C(2)−Mo(1)	175.2(3)	N(3)−C(3)−Mo(1)	178.7(5)
N(4)−C(4)−Mo(1)	176.7(3)	C(4)−N(4)−Cu(2)	146.3(3)
N(5)−C(5)−Mo(1)	176.5(4)	N(6)−C(6)−Mo(1)	178.1(4)
N(7)−C(7)−Mo(1)	179.5(3)	N(8)−C(8)−Mo(1)	177.9(3)
N(9)−Cu(1)−N(10)	95.14(13)	N(9)^{i}−Cu(1)−N(10)	84.86(13)
N(9)−Cu(1)−N(1)	94.72(13)	N(9)^{i} −Cu(1)−N(1)	85.28(13)
N(10)−Cu(1)−N(1)	96.21(12)	N(10)^{i} −Cu(1)−N(1)	83.79(12)
C(11)−N(9)−Cu(1)	117.0(3)	C(10)−N(9)−Cu(1)	108.1(2)
C(16)−N(10)−Cu(1)	108.1(2)	C(13)−N(10)−Cu(1)	119.8(3)
N(12)−Cu(2)−N(11)	95.20(10)	N(12)^{ii} −Cu(2)−N(11)	84.80(10)
N(12)−Cu(2)−N(4)	93.53(11)	N(12)^{ii} −Cu(2)−N(4)	86.47(11)
N(11)−Cu(2)−N(4)	94.84(10)	N(11)^{ii} −Cu(2)−N(4)	85.16(10)
C(22)−N(11)−Cu(2)	107.14(18)	C(23)−N(11)−Cu(2)	120.74(19)
C(27)−N(12)−Cu(2)	116.83(19)	C(28)−N(12)−Cu(2)	107.56(18)
N(14)−Cu(3)−N(13)	84.63(11)	N(14)^{iii} −Cu(3)−N(13)	95.37(11)
C(34)−N(13)−Cu(3)	107.85(19)	C(33)−N(13)−Cu(3)	119.9(2)
C(39)−N(14)−Cu(3)	108.58(19)	C(40)−N(14)−Cu(3)	117.1(2)

[a] Symmetry transformations used to generate equivalent atoms: (i) −*x* + 1, −*y* + 1, −*z*; (ii) −*x*, −*y* + 1, −*z* + 1; (iii) −*x* + 1, −*y*, −*z* + 1.

---

(15) (a) Suh, M. P.; Shin, W.; Kang, S. G.; Lah, M. S.; Chung, T. M. *Inorg. Chem.* **1989**, *28*, 1602. (b) Suh, M. P.; Shin, W.; Kim, H.; Koo, C. H. *Inorg. Chem.* **1987**, *26*, 1846.

Table 4. Bond Lengths (Å) and Angles (deg) for **3**[a]

W(1)−C(4)	2.149(4)	W(1)−C(1)	2.154(5)
W(1)−C(6)	2.154(5)	W(1)−C(2)	2.156(4)
W(1)−C(7)	2.157(5)	W(1)−C(8)	2.171(4)
W(1)−C(5)	2.173(5)	W(1)−C(3)	2.173(4)
N(1)−Cu(1)	2.409(4)	N(4)−Cu(2)	2.457(4)
Cu(1)−N(10)	2.018(3)	Cu(1)−N(9)	2.052(4)
Cu(2)−N(11)	2.025(3)	Cu(2)−N(12)	2.060(3)
Cu(3)−N(13)	2.019(3)	Cu(3)−N(14)	2.052(3)
Cu(3)−N(6)	2.535(6)		

C(4)−W(1)−C(1)	120.85(18)	C(4)−W(1)−C(6)	76.55(16)
C(1)−W(1)−C(6)	140.81(19)	C(4)−W(1)−C(2)	139.92(16)
C(1)−W(1)−C(2)	76.39(17)	C(6)−W(1)−C(2)	114.20(19)
C(4)−W(1)−C(7)	74.34(18)	C(1)−W(1)−C(7)	142.06(17)
C(6)−W(1)−C(7)	73.5(2)	C(2)−W(1)−C(7)	72.60(17)
C(4)−W(1)−C(8)	71.36(15)	C(1)−W(1)−C(8)	72.62(16)
C(6)−W(1)−C(8)	143.75(17)	C(2)−W(1)−C(8)	82.06(15)
C(7)−W(1)−C(8)	81.85(17)	C(4)−W(1)−C(5)	74.40(18)
C(1)−W(1)−C(5)	72.9(2)	C(6)−W(1)−C(5)	80.1(2)
C(2)−W(1)−C(5)	143.60(18)	C(7)−W(1)−C(5)	142.8(2)
C(8)−W(1)−C(5)	106.45(17)	C(4)−W(1)−C(3)	141.91(15)
C(1)−W(1)−C(3)	74.94(16)	C(6)−W(1)−C(3)	72.41(16)
C(2)−W(1)−C(3)	74.56(15)	C(7)−W(1)−C(3)	116.02(17)
C(8)−W(1)−C(3)	143.56(15)	C(5)−W(1)−C(3)	78.94(16)
N(1)−C(1)−W(1)	179.2(4)	C(1)−N(1)−Cu(1)	152.7(4)
N(2)−C(2)−W(1)	178.2(4)	N(3)−C(3)−W(1)	179.3(4)
N(4)−C(4)−W(1)	177.2(4)	C(4)−N(4)−Cu(2)	146.7(4)
N(5)−C(5)−W(1)	179.4(4)	N(6)−C(6)−W(1)	178.2(4)
N(7)−C(7)−W(1)	177.2(5)	N(8)−C(8)−W(1)	175.1(4)
N(10)^{i} −Cu(1)−N(9)	84.80(15)	N(10)−Cu(1)−N(9)	95.20(15)
N(10)−Cu(1)−N(1)^{i}	94.36(15)	N(9)−Cu(1)−N(1)^{i}	95.97(15)
N(10)−Cu(1)−N(1)	85.64(15)	N(9)−Cu(1)−N(1)	84.03(15)
C(11)−N(9)−Cu(1)	107.9(3)	C(14)−N(9)−Cu(1)	120.8(3)
C(16)−N(10)−Cu(1)	116.6(3)	C(17)−N(10)−Cu(1)	108.5(3)
N(11)−Cu(2)−N(12)	84.88(13)	N(11)^{ii} −Cu(2)−N(12)	95.12(13)
N(11)−Cu(2)−N(4)^{ii}	86.96(14)	N(12)−Cu(2)−N(4)^{ii}	95.07(13)
N(11)−Cu(2)−N(4)	93.04(14)	N(12)−Cu(2)−N(4)	84.93(13)
C(21)−N(11)−Cu(2)	117.1(3)	C(22)−N(11)−Cu(2)	107.5(2)
C(27)−N(12)−Cu(2)	107.1(2)	C(28)−N(12)−Cu(2)	120.9(2)
N(13)^{iii} −Cu(3)−N(14)	84.72(13)	N(13)−Cu(3)−N(14)	95.28(13)
C(33)−N(13)−Cu(3)	117.3(3)	C(32)−N(13)−Cu(3)	108.5(3)
C(38)−N(14)−Cu(3)	108.0(3)	C(35)−N(14)−Cu(3)	120.0(3)

[a] Symmetry transformations used to generate equivalent atoms: (i) $-x + 1, -y + 1, -z$; (ii) $-x, -y + 1, -z + 1$; (iii) $-x + 1, -y + 2, -z + 1$.

Each Cu atom adopts a distorted octahedral environment with two axial nitrogens (N_{ax}) of bridging CN groups and four equatorial nitrogens (N_{eq}) of the macrocycle L2. The Cu−N_{ax} distances in **2** are 2.416(4) Å for Cu1−N1, 2.466(3) Å for Cu2−N4, and 2.515(5) Å for Cu3−N6, whereas those in **3** are 2.409(5) Å for Cu1−N1, 2.457(6) Å for Cu2−N4, and 2.535(6) Å for Cu3−N6. Compared to the Cu−N_{eq} distance of 2.04(2) Å, these longer axial bond lengths, which are magnetically relevant, are definitely associated with the Jahn−Teller elongation. The overall Cu−N_{ax} bond distances of **2** and **3** are shorter than those of the other comparable M(V)−Cu(II) systems,[11] and as a consequence, stronger magnetic interactions may be expected. Another important structural factor to be considered is the Cu−N_{ax}−C_{ax} angle, which can be involved in the determination of the degree of orbital overlap between the CN bridges and Cu centers. The bond angles for **2** and **3** are similar, corresponding to 153.8(3) and 152.7(4)° for Cu1−N1−C1, 146.4(3) and 146.7(4)° for Cu2−N4−C4, and 140.7(4) and 139.4(5)° for Cu3−N6−C6, respectively. Thus, it is noticed that the bond lengths in this system are shorter than those in octacyanometalate-based M(V)−Cu(II) complexes chelated by other macrocyclic ligands.[12] As depicted in Figure S1, this feature is mainly caused by the presence of the pendant ethyl groups on the macrocycle L2, relatively located in a torsion angle (76.3(3)°) of Cu3−N13···C33−C32, which in turn serves as a source of the variation in the Cu−N_{ax} bond lengths and nonlinearity on the Cu−N_{ax}−C_{ax} angle.

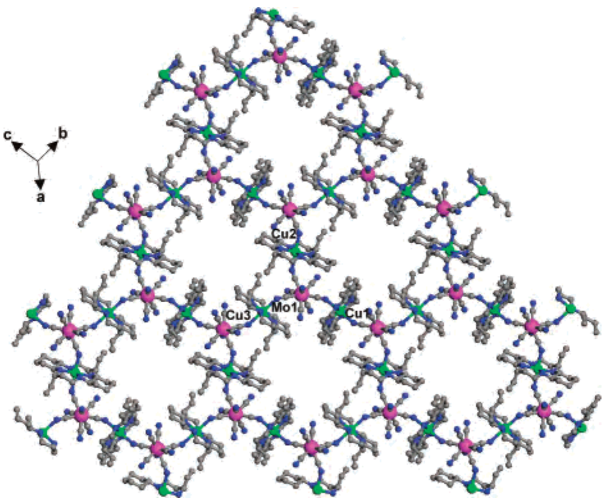

Figure 3. 2D extended layer structure of **2** illustrating a honeycomblike structure.

Figure 3 illustrates the extended molecular view of **2** portraying a fascinating honeycomblike structural type, which is also found in those of hexacyanometalate-based bimetallic assemblies.[16] The edge distances between M atoms in an irregular hexagon are in the range from 10.9104 to 11.1101 Å for **2** and from 10.9153 to 11.0990 Å for **3**. The diagonal M centers in the same hexagon are separated with distances spanning from 19.6980 to 23.6564 Å for **2** and from 19.6396 to 23.6515 Å for **3**. The layer structure is ascertained by the side view, shown in Figure S2. The shortest interlayer M−Cu distances are 9.1558(3) Å for **2**, and 9.2062(2) Å for **3**, respectively. Hydrogen bonds are formed among the nitrogen atoms of CN ligands, oxygen atoms of water/methanol molecules, and secondary amines of L2 with distances in the range of 2.546−3.407 Å for **2** and 2.900−3.426 Å for **3**.

Magnetic Properties. The magnetic susceptibility data for **2** and **3** were collected in a magnetic field of 1000 G and plotted in Figures 4 and 5. The $\chi_m T$ values are equal to 1.93 (**2**) and 1.90 cm^3 K mol^{-1} (**3**) at 300 K, which are consistent with the spin-only value (1.88 cm^3 K mol^{-1}) expected for two noninteracting M(V) ($S_M = 1/2$) and three Cu(II) ($S_{Cu} = 1/2$) ions. $\chi_m T$ increases slowly upon cooling, and then it increases sharply at low temperatures, reaching 3.73 cm^3 K mol^{-1} for **2** and 6.89 cm^3 K mol^{-1} for **3** at 1.8 K. The maximum value in **3** is larger than the expected one (4.38 cm^3 K mol^{-1}) for $S_T = 5/2$ of a ferromagnetic Cu_3M_2 unit, while the peak value in **2** is smaller. This suggests that short-range ferromagnetic interactions in **2** and the extended correlation length through the layer in **3** are involved at 1.8 K. The fitting of the inverse magnetic susceptibility data with the Curie−Weiss law, $\chi_m = C/(T - \theta)$, gives parameters of $C = 1.91$

---

(16) (a) Kou, H.-Z.; Gao, S.; Bai, O.; Wang, Z.-M. *Inorg. Chem.* **2001**, *40*, 6287. (b) Ohba, M.; Okawa, H.; Fukita, N.; Hashimoto, Y. *J. Am. Chem. Soc.* **1997**, *119*, 1011. (c) Hong, C. S.; You, Y. S. *Inorg. Chim. Acta* **2004**, *357*, 3271.

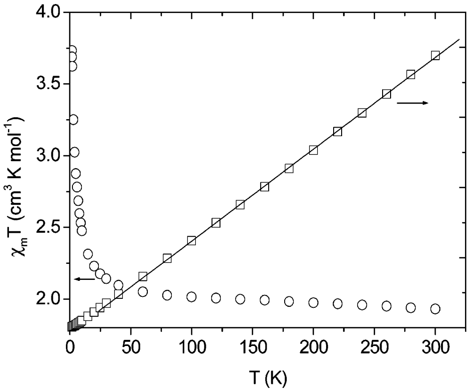

Figure 4. Plots of $\chi_m T$ and $1/\chi_m$ vs T for **2**·6H$_2$O. The solid line shows the best theoretical fit.

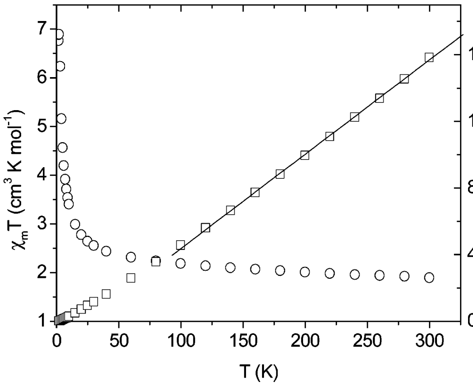

Figure 5. Plots of $\chi_m T$ and $1/\chi_m$ vs T for **3**·6H$_2$O·MeOH. The solid line presents the best theoretical fit.

cm^3 K mol^{-1}, $\theta = 5.68$ K ($T > 60$ K) for **2** and $C = 1.77$ cm^3 K mol^{-1}, $\theta = 23.0$ K ($T > 120$ K) for **3**. The positive Weiss constants (θ) demonstrate that the ferromagnetic interactions between neighboring Cu(II) and M(V) spins in the lattice are dominating. The obtained θ values for **2** and **3** are higher than those for other Cu(II)−M(V) systems with longer Cu−N$_{ax}$ bond lengths.[12] It is worth noting that the Weiss constant of **3** is much larger than that of **2**, signaling the operation of stronger ferromagnetic exchange couplings between Cu(II) and W(V) spins through the CN linkage rather than through the Cu−Mo pair. One plausible reason for the observed enhanced magnetic strength in **3** emanates from the fact that the 5d orbital on W(V) is more diffuse than the 4d orbital on M(V).[17]

Figures 6 and 7 display the field dependence of the magnetization in **2** and **3**. The magnetization per Cu$_3$M$_2$ increases rapidly with increasing field and saturates to values of 4.93 Nβ (**2**) and 5.41 Nβ (**3**), which are close to the expected one (5 Nβ with $g = 2$). The experimental curves at several temperatures are always higher than those derived from the Brillouin function, confirming that the Cu(II) and M(V) spins are ferromagnetically coupled at that temperature. Thus, the M(T) and M(H) data clearly demonstrate that under the given structural environments the CN bridge mediates global ferromagnetic arrangements through the lattice.

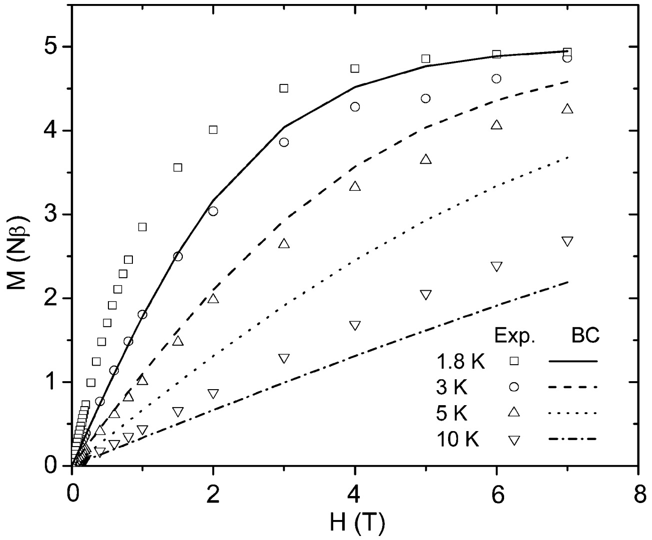

Figure 6. Field dependence of the magnetization of **2**·6H$_2$O. The Brillouin curves (BC) for three independent Cu(II) and two Mo(V) ions are given at various temperatures.

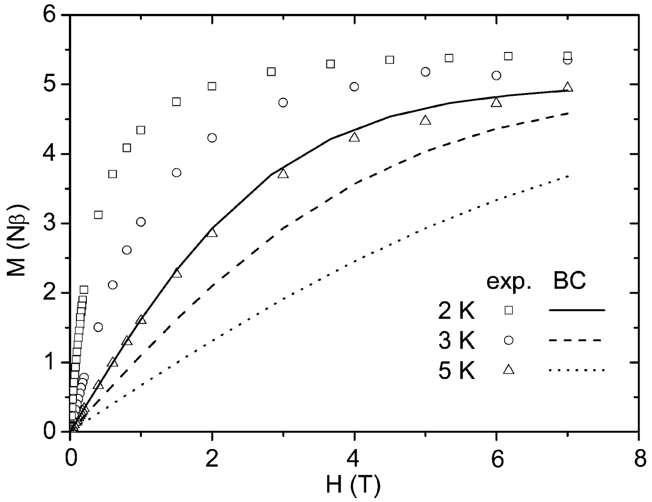

Figure 7. Field dependence of the magnetization of **3**·6H$_2$O·MeOH. The Brillouin curves (BC) for three isolated Cu(II) and two W(V) ions are drawn at various temperatures.

The total exchange coupling constant (J) can be expressed as $J = J_F$ (ferromagnetic term) $+ J_{AF}$ (antiferromagnetic term) $= 2k$ (>0) $+ 4\beta S$ (<0), where S is the overlap integral.[18] The J value will be positive if J_F, depending on k, predominates over J_{AF}, proportional to S. This can be accomplished on the condition of S being quite small or close to zero. This situation might be met because, given the Cu−N$_{ax}$ bond lengths and Cu−NC angles, the magnetic orbital ($d_{x^2-y^2}$) on Cu(II) atom located in the basal plane of L2 does not propagate effectively through the empty π^* orbitals of the CN bridges that overlap in a π pathway with the orbitals (d_{z^2}:$d_{x^2-y^2}$) of neighboring M(V) atoms.[19] Provided that ferromagnetic interactions are operative in this system, it is conceivable that the overlap (S) between magnetic orbitals of Cu(II) and M(V) is minimal, eventually making the sum of J_F and J_{AF} positive. Accordingly, when the Cu−N$_{ax}$ bond

---

(17) (a) Song, Y.; Ohkoshi, S.-i.; Arimoto, Y.; Seino, H.; Mizobe, Y.; Hashimoto, K. *Inorg. Chem.* **2003**, *42*, 1848. (b) Yoon, J. H.; Kim, H. C.; Hong, C. S. *Inorg. Chem.* **2005**, *44*, 7714.

(18) Kahn, O. *Molecular Magnetism*; VCH: Weinheim, Germany, 1993.

(19) Chibotaru, L. F.; Mironov, V. S.; Ceulemans, A. *Angew. Chem., Int. Ed.* **2001**, *40*, 4429.

Table 5. Structural and Magnetic Parameters for Octacyanometalate-Based M−Cu (M = Mo, W) Systems with Axial−Axial Bridging Modes Around the Cu Ions

compounds	$Cu-N_{ax}$ (Å)	$Cu-N_{ax}-C_{ax}$ (deg)	θ (K)	ref
$[Cu(cyclam)]_3[Mo(CN)_8]_2\cdot 5H_2O$	2.514−2.711	142.7−160.6	1.24	12a
$[Cu(en)_2]_3[W(CN)_8]_2\cdot H_2O$	2.534−2.731	115.7−143.0	1.96	20
$[Cu(L)]_3[Mo(CN)_8]_2\cdot 6H_2O$	2.548−2.583	135.7−157.8	2.0	12b
$[Cu(L)]_3[W(CN)_8]_2\cdot 6H_2O$	2.572−2.607	137.4−159.2	3.9	12b
2	2.416−2.515	140.7−153.8	5.68	this work
3	2.409−2.535	139.4−152.7	23.0	this work

length is sufficiently long, as in this system, the variation of $Cu-N_{ax}-C_{ax}$ angle may not influence the magnetic character in systems with an axially elongated octahedral Cu(II) ion and $[M(CN)_8]^{3-}$ (M = Mo, W) bridged by CN anions,[12,20] as shown in Table 5. The magnitude of magnetic exchange coupling tends to increase as the $Cu-N_{ax}$ bond length shortens, which is a consequence of competing J_{AF} and J_F terms.[18]

Conclusions

A new molecular precursor Cu(II) (**1**) complex with a macrocyclic ligand L2 containing the ethyl pendant groups has been devised and employed in the construction of cyano-bridged $Cu^{II}-M^V$ [M = Mo (**2**), W (**3**)] bimetallic systems via a self-assembly process. Both compounds reveal an aesthetic structural pattern of honeycomblike two-dimensional sheets. The pendant groups on the macrocycle discernibly affect the variation of $Cu-N_{ax}$ bond length and $Cu-N_{ax}-C_{ax}$ bond angles. The magnetic studies demonstrate that global ferromagnetic interactions occur under the given structural parameters. From these magnetic results, when the $Cu-N_{ax}$ bond length in axially elongated octahedral Cu(II) geometry is long enough, the prevalent ferromagnetic nature appears to be maintained despite the broad range of the $Cu-N_{ax}-C_{ax}$ angle.

Acknowledgment. This work was supported by a Korea Research Foundation Grant funded by the Korean government (MOEHRD, Basic Research Promotion Fund) (KRF-2005-070-C00068) and CRM-KOSEF. We also thank an Operation Program on Shared Research Equipment of KBSI and MOST.

Supporting Information Available: Relevant crystal structures of **2** (Figures S1 and S2) and crystallographic information in CIF format. This material is available free of charge via the Internet at http://pubs.acs.org.

IC060868B

---

(20) Li, D.-F.; Gao, S.; Zheng, L.-M.; Sun, W.-Y.; Okamura, T.-a.; Ueyama, N.; Tang, W.-X. *New J. Chem.* **2002**, *26*, 485.